MEGA JOURNAL OF CASE REPORTS

Research Article

Published Date: November 09, 2022

Exploring the Mechanism of the Cystic Fibrosis Transmembrane Conductance Regulator-ATP Binding Through Molecular Dynamics and Potential of Mean Force Simulations

Xin Li[1#*] and Xinguan Tan[2#]

[1]Chongqing Key Laboratory of Theoretical and Computational Chemistry, School of Chemistry and Chemical Engineering, Chongqing University, PR China

[2]College of Mathematics and Physics, Chengdu University of Technology, PR China

[#]Two authors contributed equally to this work.

[*]**Corresponding author**: Xin Li, Chongqing Key Laboratory of Theoretical and Computational Chemistry, School of Chemistry and Chemical Engineering, Chongqing University, Chongqing, 401331, PR China, Tel: +86-17708315861; E-mail: lixinxin@cqu.edu.cn

Abstract

The cystic fibrosis transmembrane conductance regulator (CFTR) is an anion channel important in maintaining proper functions of the lung, pancreas, liver, kidneys, and intestine. The activity of CFTR is regulated by ATP and protein kinase A-dependent phosphorylation. However, there is little published data on the interaction between ATPs and CFTRs. In this work, the classical molecular dynamic simulations and then the hydrogen bonds analysis were carried out to investigate the interaction between ATPs and CFTRs for the phosphorylated/dephosphorylated CFTR-ATP1/ATP2 complexes. The followed potential of mean force (PMF) simulations were performed to determine the free energy profiles. A significant free energy barrier (~1 kcal/mol) exists in the phosphorylated/dephosphorylated CFTR-ATP1 binding process. This research sheds new light on the mechanism of ATP-binding in CFTR.

Keywords: CFTR; Molecular dynamic; Potential of mean force; Hydrogen bond; Energy barrier

Introduction

Cystic Fibrosis (CF), a genetic disorder that affects mostly the lungs, but also the pancreas, liver, kidneys, and intestine, is caused by mutations in the gene encoding the Cystic Fibrosis Transmembrane Conductance Regulator (CFTR) protein **[1-3].** Even with modern medical care, the average survival age of cystic fibrosis patients is ~ 40 y old **[3].** As a membrane protein and chloride channel, CFTR contains two Transmembrane Domains (TMDs), each with six spans of alpha helices, which are each connected to a Nucleotide Binding Domain (NBD) in the cytoplasm. The first NBD is connected to the second transmembrane domain by a regulatory "R" domain that is a unique feature of CFTR, not present in other ATP-Binding Cassette (ABC) transport proteins **[4].** The CFTR ion channel only opens when its R-domain has been phosphorylated by Protein Kinase A (PKA) and ATP is bound at the NBDs. ATP binds to each nucleotide binding domain, which results in the subsequent NBD dimerization, leading to the transition from an inward-facing conformation to an outward-facing one **[5].** Based on the structures of phosphorylated and dephosphorylated chicken CFTR determined by Fay et al. with the cryo-EM method **[2],** we carried out Molecular Dynamics (MD) and Potential Of Mean Force (PMF) simulations to determine the free energy profiles of the CFTR-ATP binding process. The combined MD and PMF simulations have revealed some interesting details of the mechanism of ATP-binding.

Methods

MD simulation

The phosphorylated and dephosphorylated chicken CFTR structures, both ATP-bound, are from the RCSB protein database (http://www.rcsb.org/pdb, PDB ID:6D3S and 6D3R respectively) **[2].** CHARMM-GUI was used to build the model of the two protein structures inserted into DOPC lipid bilayer **(Figure S1).** For clarity, the two ATPs are referred as ATP1 and ATP2 respectively **(Figure S2 and S3).**

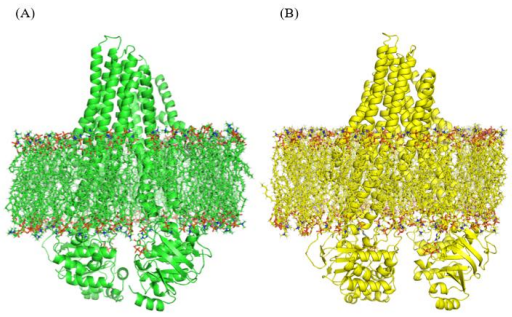

Figure S1: The complex structures of the phosphorylated CFTR-ATP1/ATP2 (A) and the dephosphorylated CFTR-ATP1/ATP2 (B) inserted into DOPC lipid bilayer. For clarity, the water shell is hidden.

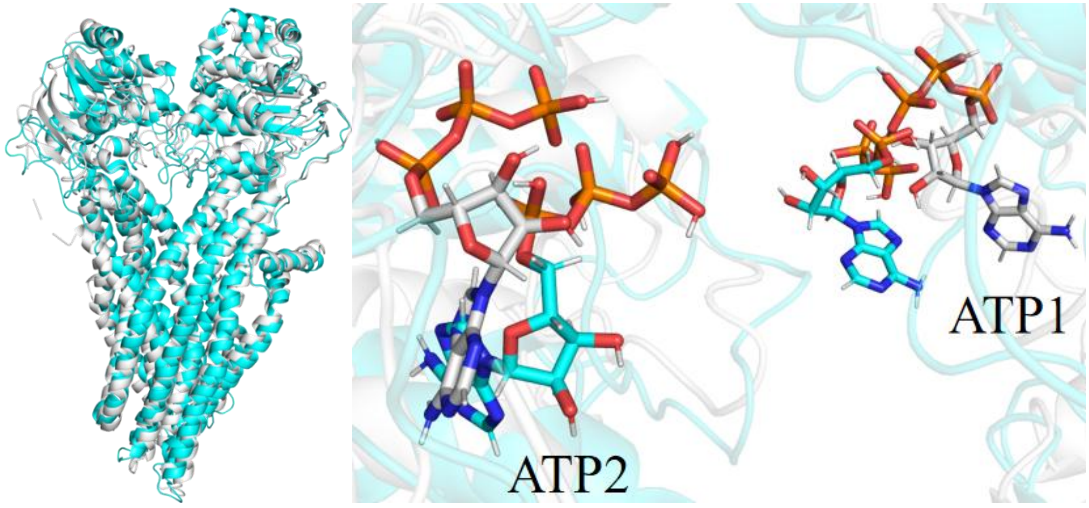

Figure S2: Superimposition of the last snapshot (cyan) of the 100ns production simulation of the phosphorylated CFTR-ATP1/ATP2 complex to its crystal structure (gray). The protein is shown in ribbon and ATP in sticks.

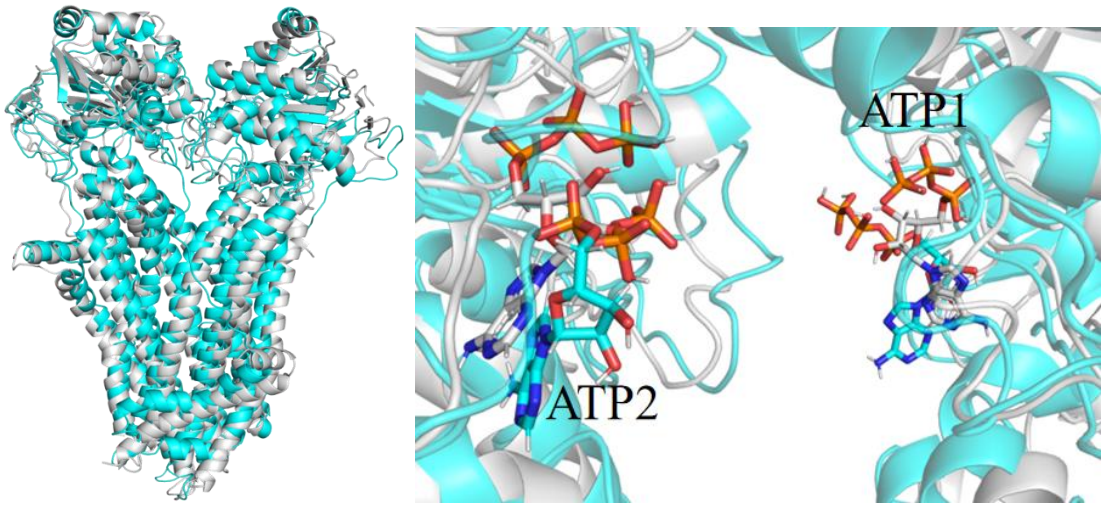

Figure S3: Superimposition of the last snapshot (cyan) of the 100ns production simulation of the dephosphorylated CFTR-ATP1/ATP2 complex to its crystal structure (gray). The protein is shown in ribbon and ATP in sticks.

MD simulation was performed by using the Sander module of the Amber 22 program package **[6-10].** For each structure, energy-minimization was performed via a combined use of the steepest descent/conjugate gradient algorithms, with a convergence criterion of 0.01 kcal·mol^{-1}Å^{-2}, and the non-bonded cutoff distance was set to 10.0 Å. The partial charges of ATP atoms were calculated by using the Restrained Electrostatic Potential-Fitting (RESP) protocol implemented in the Antechamber module, following the Electrostatic Potential (ESP) calculation at ab initio HF/6-31G* level using Gaussian 09 program **[11].** Sodium counter ions (Na+) were added to neutralize the solvated system. The solvated system was gradually heated to 298.15 K by the weak-coupling method **[12]** and equilibrated for 150 ps. During the MD simulations, a 10.0 Å non-bonded interaction cutoff was used and the non-bonded list was updated every 25 steps. The motion for the mass center of the system was removed every 1000 steps. The Particle-Mesh Ewald (PME) method **[13,14]** was used to treat long-range electrostatic interactions. The lengths of covalent bonds involving hydrogen atoms were fixed with the SHAKE algorithm **[15],** enabling the use of a 2-fs time step to numerically integrate the equations of motion. Finally, the production MD was kept running for 100ns with a periodic boundary condition in the NTP ensemble at T=298.15 K with Berendsen temperature coupling, and at P=1 atm with isotropic molecule-based scaling **[16].** In the energy-minimization and heating procedures all of the ATP, protein and lipid atoms were restrained by a harmonic potential with a force constant of 2000 kcal·mol^{-1}Å^{-2}. The following NPT equilibration simulation

divided into 6 steps: (1) 100ps, all of the ATP, protein and lipid atoms were restrained; (2) 100ps, the atoms of the protein were restrained; (3) 100ps, the main chain atoms of the protein were restrained; (4) 100ps, the backbone atoms of the protein were restrained; (5) 100ps, the Calpha atoms of the protein were restrained; (6) 100ps, none of the systems was restrained. The harmonic potential used in equilibration simulation was the same as that used in energy-minimization and heating procedures. Hydrogen bonds analysis were based on the production simulation trajectory. The criterion for forming a hydrogen bond was that the distance between the heavy atoms was no larger than 3.0Å and the angle between the acceptor, hydrogen, and donor atoms was no smaller than 135 degree.

Potential of mean force (PMF) simulation

In order to explore the free energy profiles for the process of ATP binding with CFTR, the PMF simulation was carried out by using umbrella-sampling [17] MD simulation. The classic PMF definition [18] can be represented by a function of reaction coordinate as

$$\omega(\chi) = -RT \ln\langle \rho(\chi)\rangle - U(\chi) + F$$

in which ρ(χ) is the probability density along the reaction coordinate χ, R is the gas constant, T is the simulation temperature, U(χ) is the biasing potential applied in the umbrella-sampling MD simulation, and F is the normalization constant. According to this approach, the reaction coordinate is usually divided into different regions, i.e., windows, and each window is sampled separately. A biasing (umbrella) potential, i.e. U(χ), is applied for each window in order to obtain nearly uniform sampling of the potential energy surface. In the present study, the reaction coordinate was defined as the distance from the mass center of the non-hydrogen atoms of the ATP molecular to the mass center of the C_{alpha} atoms of several residues of CFTR, which participate in hydrogen bond interactions with ATPs. For the phosphorylated CFTR-ATP complex, residues Glu1373, Arg1247, Tyr1221 and Gln533 were chosen for ATP1, and residues Glu665 and Arg 669 were chosen for ATP2. For dephosphorylated CFTR-ATP complex, residues Glu1419, Arg1247 and Thr1254 were chosen for ATP1 and Asp174, Leu1063 and Trp1067 were chosen for ATP2. We can speculate the direction of the unbinding process based on the knowledge of the structures, and the above residues are in the opposite direction. The total number of windows was 21, with a window size of 0.3 Å. The biasing force constant applied in different windows of umbrella-sampling was 10.0 kcal/(mol·Å). For each umbrella-sampling window, the initial complex structure was selected from the last snapshot of the PMF simulations of the previous window. The selected structure for each window was first equilibrated for 200 ps and then kept running

for 800 ps for production sampling. The frequency for data collection was set to 1 fs, which was the same as that of the time step of the umbrella-sampling MD. After the umbrella-sampling MD simulations for all windows were completed, the data collected from separate simulation windows were combined along the reaction coordinate. These data were then used to calculate the PMF for the whole binding process with the Weighed Histogram Analysis Method (WHAM) **[19,20]** using the code developed by Alan Gross field (http://membrane.urmc.rochester.edu/?page_id=126).

Results and Discussion

Hydrogen bonds analyses based on trajectories of classical MD

The Root Mean Square Deviation (RMSD) of the protein backbone atoms shows that the systems are very stable after about 30ns simulation **(Figure 1).** Therefore, we chose the 30-100ns simulation trajectory for hydrogen bonds analyses. And as shown in **Figure S2 and S3,** which are the structure in the last snapshot of the both MD simulated CFTR complexes aligned to the initial structures, the structures experienced reasonable conformational change during 100ns MD simulation.

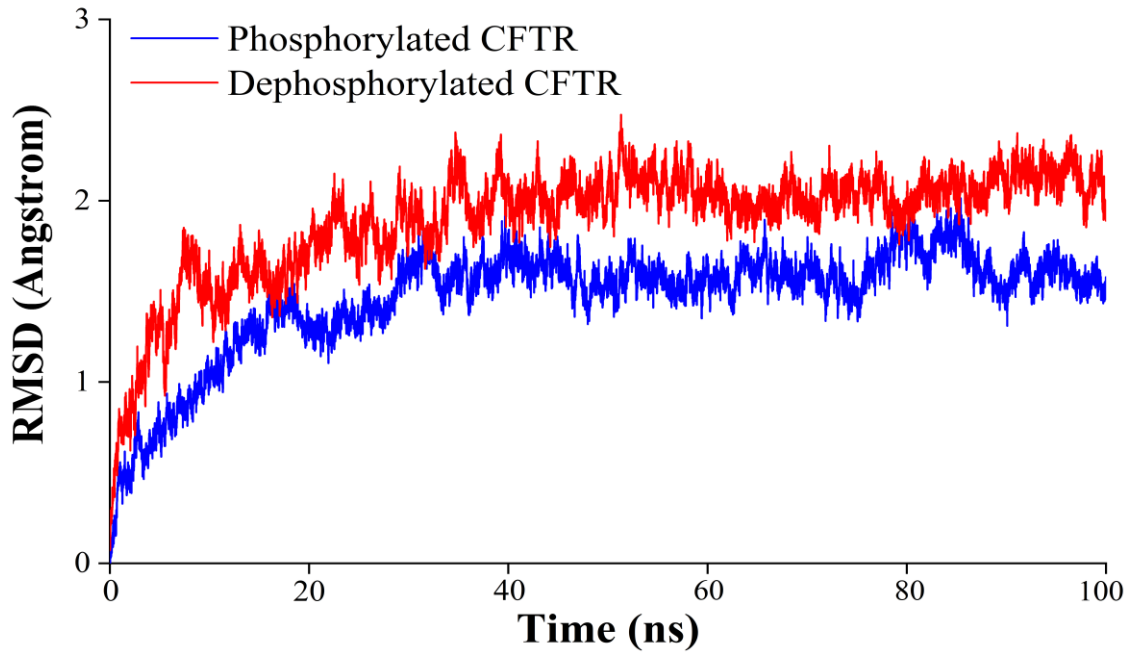

Figure 1: Backbone RMSD (Root-Mean-Square Deviation) of the phosphorylated CFTR (blue) and the dephosphorylated CFTR (red) during the simulation.

According to the hydrogen bonds analyses of MD-simulated phosphorylated CFTR complex, a very stable hydrogen bonding network is formed between CFTR-ATP1 and residues Glu1373, Gln553, Ser1250, Arg1247, Tyr1221, Gly1249 **(Figure 2A),** with the total occupancy of 99.8%, 64.4%, 58.4%, 57.9%, 36.0% and 16.4% respectively, sorted from highest to lowest **(Table 1).** Among these hydrogen bonds, the strongest is the one composed of the OE2 atom of Glu1373 and the O8 atom of CFTR-ATP1, whose occupancy approximates 100%. The average distance is 2.58Å and the average angle is 167 degrees for this hydrogen bond. CFTR-ATP2' hydrogen bonding network relates only to two residues, one is Arg669 with the occupancy of 63.6% and the other is Glu665 with the occupancy of 45.2%. Not only in quantity but also the individual occupancy, the latter hydrogen bonding network is much unstable than the former.

Table 1: Hydrogen bond analysis with the equilibrium trajectories of the phosphorylated CFTR-ATP1/ATP2 complex.

Acceptor	Donor	Occupancy (%)	Average Distance(Å)	Average Angle(°)
Glu_1373@OE2	ATP1_1442@O8	99.80	2.58	167.24
Gln_553@OE1	ATP1_1442@O3	37.15	2.79	155.46
ATP1_1442@O4	Gln_553@NE2	27.21	2.88	161.35
Ser_1250@O	ATP1_1442@O7	29.33	2.68	159.25
ATP1_1442@O10	Ser_1250@N	29.07	2.86	157.86
Arg_1247@O	ATP1_1442@O7	57.93	2.66	164.89
ATP1_1442@O6	Tyr_1221@OH	36.01	2.73	163.42
ATP1_1442@O10	Gly_1249@N	16.40	2.83	147.46
ATP2_1443@O5	Arg_669@NH2	52.33	2.81	153.04
ATP2_1443@O10	Arg_669@NH2	11.34	2.80	155.66
Glu_665@OE1	ATP2_1443@O13	19.74	2.57	168.14
Glu_665@OE2	ATP2_1143@O13	13.04	2.57	167.56
Glu_665@OE2	ATP2_1143@O4	12.42	2.66	164.38

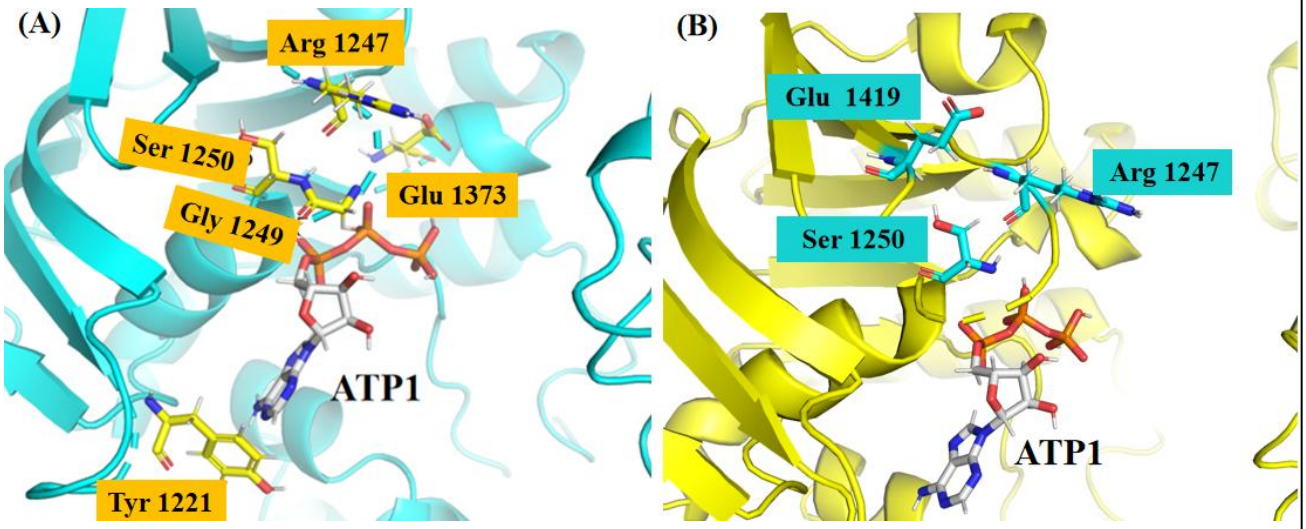

Figure 2: The residues participating in the hydrogen bonding network for ATP1 (A) of the phosphorylated CFTR-ATP1/ATP2 complex and ATP1 (B) of the dephosphorylated CFTR-ATP1/ATP2 complex. The residues and ATPs are in sticks.

The hydrogen bonds for the ATP1/dephosphorylated CFTR are quite similar to that of the ATP1/phosphorylated CFTR, both containing the same residues of Arg1247, Ser1250 and one similar Glu residue (Glu1419) **(Table 2 and Figure 2B).** However, the situation for the CFTR-ATP2 is opposite. There is no consistent residue participating in the CFTR-ATP2' hydrogen bonding network. Except for three residues (Asp174, Leu1063, Trp1067) participating in the hydrogen bonding network of the ATP2/dephosphorylated CFTR, which locate at the bottom of the TMD, all of the hydrogen-bonding-network-relating residues are included in the NBD. This is in accordance with current knowledge that in the phosphorylated CFTR complex, ATP binds to each nucleotide binding domain, triggering the subsequent NBD dimerization, leading to the transition from an inward-facing conformation to an outward-facing one. Maybe the conformational change in the dephosphorylated CFTR complex will impede this transition through different mechanism of hydrogen bonding network.

Table 2: Hydrogen bond analysis with the equilibrium trajectories of the dephosphorylated CFTR-ATP1/ATP2 complex.

Acceptor	Donor	Occupancy (%)	Average Distance(Å)	Average Angle(°)
Glu_1419@OE1	ATP1_1442@O10	99.34	2.56	167.57
Glu_1419@OE2	ATP1_1442@O11	99.12	2.60	167.39
ATP1_1442@O5	Arg_1247@NH1	75.40	2.82	158.41
Thr_1254@OG1	ATP1_1442@O5	15.44	2.79	160.42
ATP1_1442@O4	SER_1250@OG	10.26	2.81	157.29
Asp_174@OD2	ATP2_1443@O12	55.35	2.63	161.42
Leu_1063@O	ATP2_1443@O11	19.84	2.66	161.62
ATP2_1443@O5	Trp_1067@NE1	13.92	2.89	159.57
ILE_663@O	ATP2_1443@N3	11.06	2.85	156.77

Depicted in **Figure S4-S7** are distances and angles for important hydrogen bonds around ATPs during 100ns MD simulations in phosphorylated and dephosphorylated chicken CFTR structures.

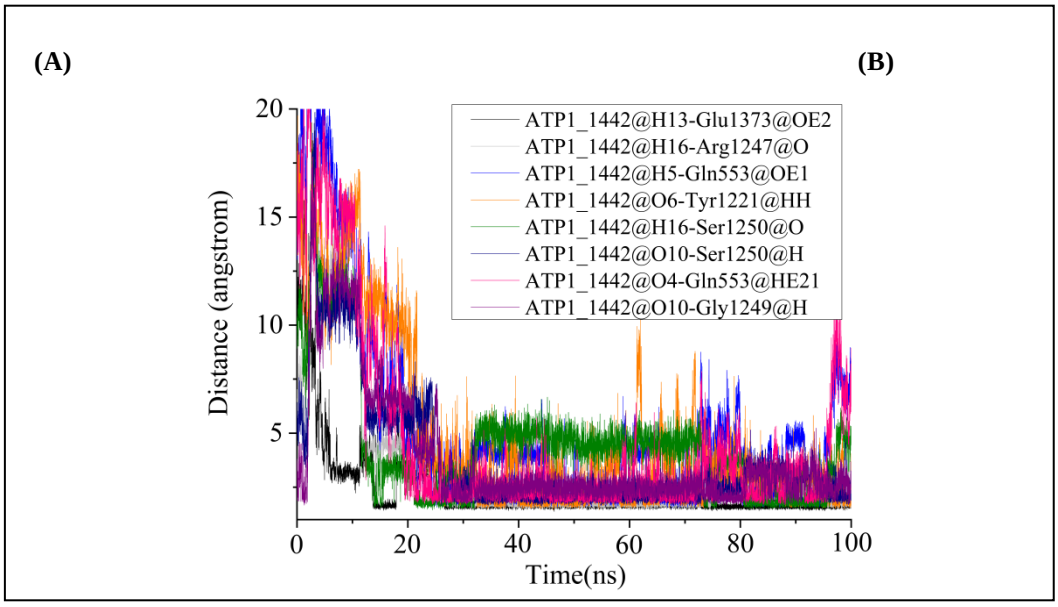

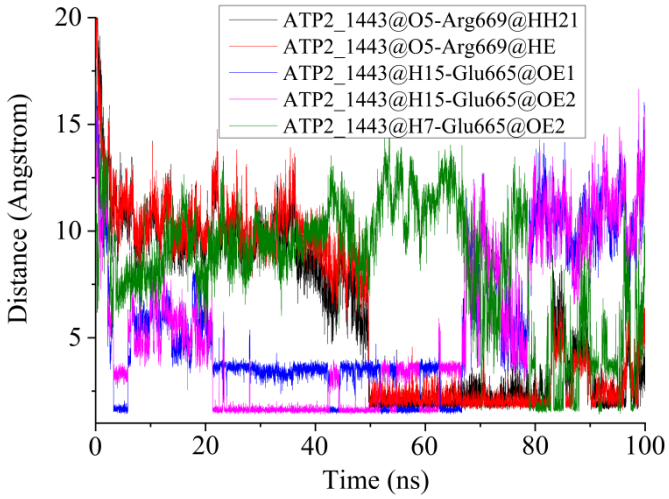

Figure S4: (A) Hydrogen bonds distances for ATP1 of the phosphorylated CFTR-ATP1/ATP2 complex. (B) Hydrogen bonds distances for ATP2 of the phosphorylated CFTR-ATP1/ATP2 complex.

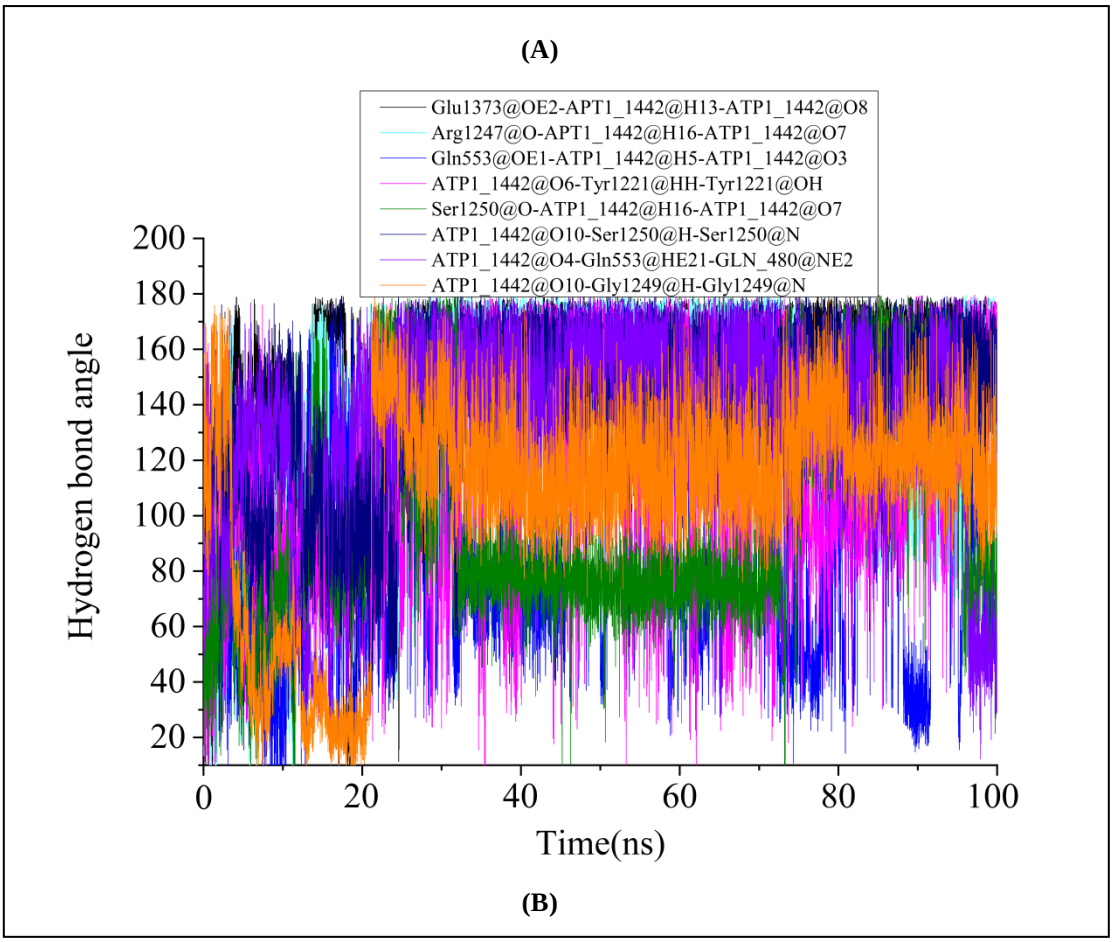

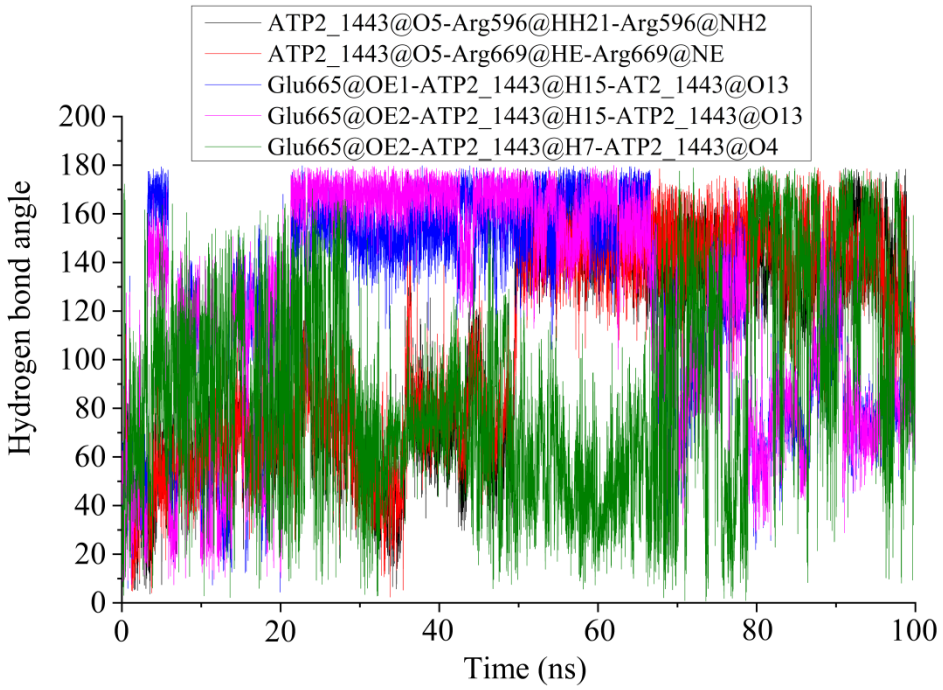

Figure S5: (A) Hydrogen bonds angles for ATP1 of the phosphorylated CFTR-ATP1/ATP2 complex. (B) Hydrogen bonds angles for ATP2 of the phosphorylated CFTR-ATP1/ATP2 complex.

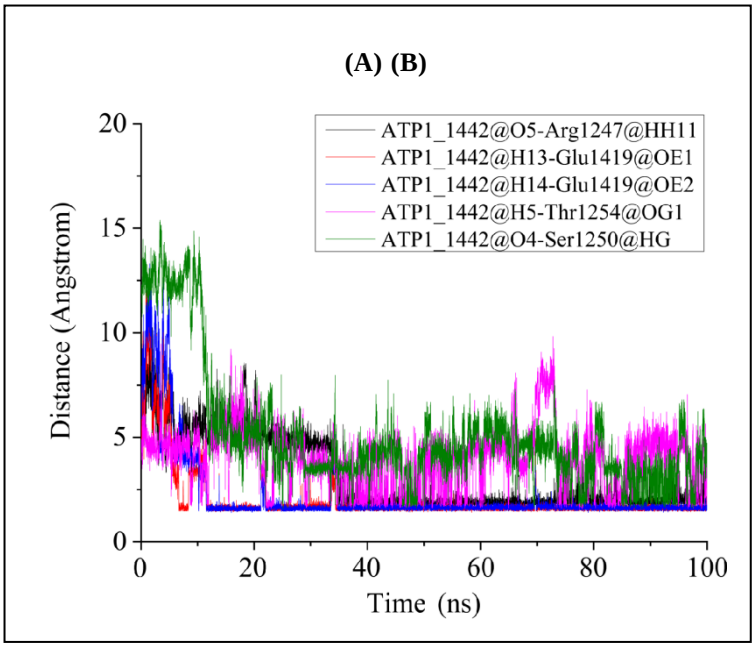

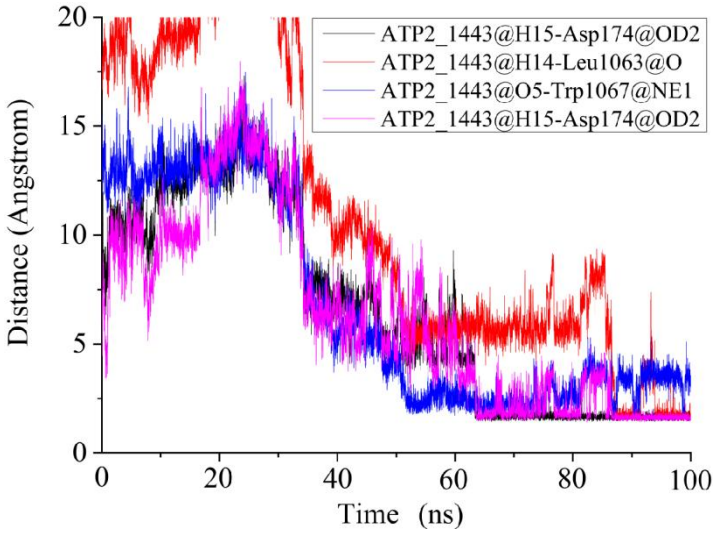

Figure S6: (A) Hydrogen bonds distances for ATP1 of the dephosphorylated CFTR-ATP1/ATP2 complex. (B) Hydrogen bonds distances for ATP2 of the dephosphorylated CFTR-ATP1/ATP2 complex.

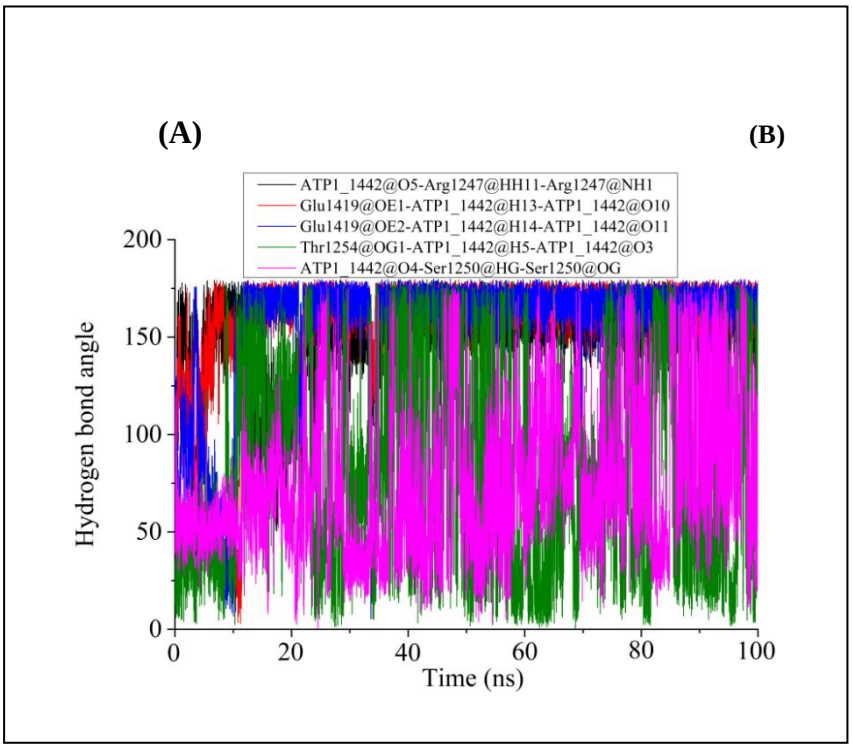

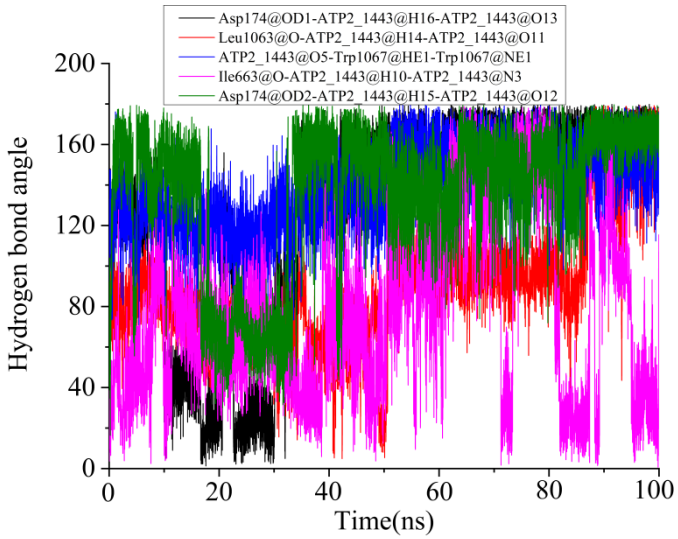

Figure S7: (A) Hydrogen bonds angles for ATP1 of the dephosphorylated CFTR-ATP1/ATP2 complex. (B) Hydrogen bonds angles for ATP2 of the dephosphorylated CFTR-ATP1/ATP2 complex.

Free energy profiles of the phosphorylated/dephosphorylated CFTR-ATP1/ATP2 binding processes simulations

Depicted in **Figure 3** are the PMF free energy profiles **[21,22]** obtained for the phosphorylated/dephosphorylated CFTR-ATP1/ATP2 binding processes. In terms of the equilibrium phosphorylated/dephosphorylated CFTR-ATP1/ATP2 binding, the free energy profiles depicted in **Figure 3** indicate that the calculated binding free energy is 7.7 kcal/mol for phosphorylated CFTR-ATP1, 5.9 kcal/mol for phosphorylated CFTR-ATP2, 3.9 kcal/mol for dephosphorylated CFTR-ATP1 and 1.7 kcal/mol for dephosphorylated CFTR-ATP2. Both in phosphorylated and dephosphorylated CFTR, the calculated binding free energy for ATP2 is remarkably lower than that for ATP1 (about 1.8 kcal/mol and 2.2 kcal/mol, respectively), indicating that one binding site is more favorable than the other. This is consistent with our previous conclusion that hydrogen bonding network of ATP2 is much unstable than that of ATP1. In general, it seems that ATPs bind much more tightly to the phosphorylated CFTR (with quantitatively much higher binding free energy), relative to the dephosphorylated CFTR. According to previous studies, the CFTR ion channel only opens when its R-domain has been phosphorylated by Protein Kinase A (PKA) and ATP is bound at the NBDs. Maybe the phosphorylation of the CFTR is beneficial for ATP binding.

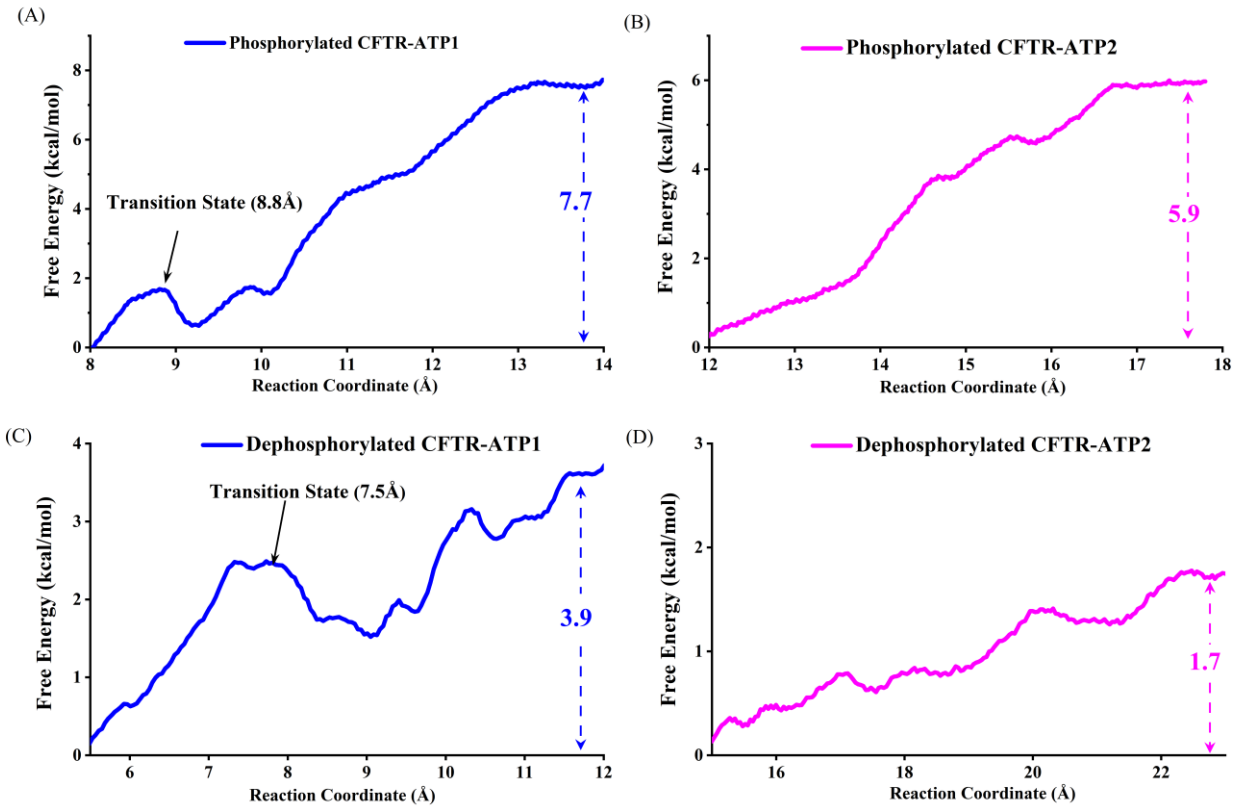

Figure 3: Simulated free energy profiles for the phosphorylated/dephosphorylated CFTR-ATP1/ATP2 binding processes.

Interestingly, it seems that there are characteristic significant free energy barriers of ATP1 binding to the CFTR in general, either the phosphorylated CFTR or the dephosphorylated CFTR, whereas no such free energy barriers found in the phosphorylated/dephosphorylated CFTR-ATP2 binding processes. The free energy barrier appears at χ = ~8.8 Å and χ = ~7.5Å respectively for the phosphorylated/dephosphorylated CFTR-ATP1 binding process. And the two free energy barriers are both about 1kcal/mol. The free energy barrier is associated with conformational adjustment of the ATP1 near the binding site. For the phosphorylated CFTR-ATP1 complex, the adenine and sugar groups of the ATP1 remain unchanged, while the triphosphate group of the ATP1 undergoes a dramatic torsion for the following possible binding at appropriate site **(Figure 4).** To the contrary, for the dephosphorylated CFTR-ATP1 complex, the adenine and sugar groups undergoes a dramatically torsion while the triphosphate group remain unchanged. It is reasonable to speculate that ATP1 modulates its orientation before arriving the binding site for following best binding to CFTR when arriving the binding site.

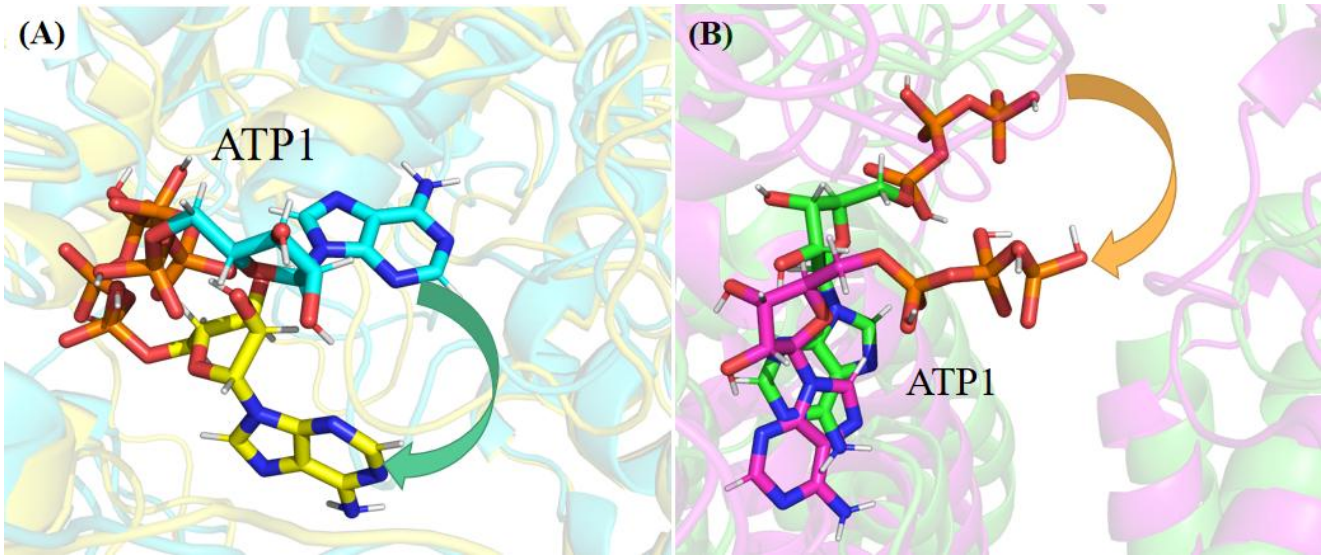

Figure 4: (A)The torsion of the adenine and sugar groups of the ATP1 in the phosphorylated CFTR-ATP1 binding process at the transition state (when χ = ~8.8 Å). The structures right before χ = ~9.0 Å) and after (χ = ~8.5 Å) the transition state are shown in cyan and yellow respectively. (B) The torsion of the triphosphate group of the ATP1 in the dephosphorylated CFTR-ATP1 binding process at the transition state (when χ = ~7.5 Å). The structures right before (χ = ~7.8 Å) and after (χ = ~7.2 Å) the transition state are shown in green and magenta respectively.

Conclusion

The combined MD and PMF simulations have led to determination of the hydrogen bonding network and the free energy profiles of the phosphorylated/dephosphorylated CFTR-ATP1/ATP2 binding processes. Both the hydrogen bonds analyses and the free energy profiles indicate that the ATP1 binding site is more favorable than the ATP2 binding site. ATPs bind much more tightly to the phosphorylated CFTR (with quantitatively much higher binding free energy), relative to the dephosphorylated CFTR. According to the obtained free energy profiles, a significant free energy barrier (~1 kcal/mol) exists in the phosphorylated/dephosphorylated CFTR-ATP1 binding processes, whereas no obvious free energy barrier exists in the phosphorylated/dephosphorylated CFTR-ATP2 binding processes. We speculate that the free energy barrier is associated with the orientation/conformation adjustment of ATP1 near the binding site. Our results may be beneficial for further study in the ATP-gating mechanism of CFTR.

References

1. Clancy JP, Cotton CU, Donaldson SH, et al. CFTR modulator theratyping: Current status, gaps and future directions. J Cyst Fibros. 2019;18(1):22-34.
2. Fay JF, Aleksandrov LA, Jensen TJ, et al. Cryo-EM Visualization of an Active High Open Probability CFTR Anion Channel. Biochemistry. 2018;57(43):6234-46.
3. Zhang Z, Liu F, Chen J. Molecular structure of the ATP-bound, phosphorylated human CFTR. PNAS.2018;115(50):12757-62.
4. Sheppard DN, Welsh MJ. Structure and function of the CFTR chloride channel. Physiol Rev. 1999;79(1):S23-45.
5. Csanády L, Vergani P, Gadsby DC. Structure, Gating, and Regulation of the CFTR Anion Channel. Physiol Rev. 2019;99(1):707-38.
6. Pearlman DA, Case DA, Caldwell JW, et al. AMBER, a package of computer programs for applying molecular mechanics, normal mode analysis, molecular dynamics and free energy calculations to simulate the structural and energetic properties of molecules. Comput Phys Commun. 1995;91(1-3):1-41.
7. Case DA, Cheatham TEIII, Darden T, et al. The Amber Biomolecular Simulation Programs. J Comput Chem. 2005;26(16):1668-88.
8. Frank M, Gutbrod P, Hassayoun C, et al. Dynamic molecules: molecular dynamics for everyone. An internet-based access to molecular dynamic simulations: basic concepts. J Mol Model. 2003;9(5):308-15.
9. Karplus M. Molecular Dynamics of Biological Macromolecules: A Brief History and Perspective. Biopolymers. 2003;68(3):350-8.
10. Adcock SA, Mccammon JA. Molecular Dynamics: Survey of Methods for Simulating the Activity of Proteins. Chem Rev. 2006;106(5):1589-615.
11. Frisch MJ, Trucks GW, Schlegel HB, et al. Gaussian 09, Gaussian Inc., Pittsburgh, PA, 2009.
12. Morishita T. Fluctuations fromulas in molecular dynamics simulations with the weak coupling heat bath. J Chem Phys. 2000;113(8):2976-82.
13. Darden T, York D, Pedersen L. Particle mesh ewald-an N_log(N) method for ewald sums in large systems. J Chem Phys. 1993;98:10089-92.

14. Toukmaji A, Sagui C, Board J, Darden T. Efficient particle-mesh ewald based approach to fixed and induced dipolar interactions. J Chem Phys. 2000;113(24):10913-27.
15. Ryckaert JP, Ciccotti G, Berendsen HJC. Numerical-integration of cartesian equations of motion of a system with constraints-molecular dynamics of n-alkanes. J Comput Phys. 1997;23(3):327-41.
16. Berendsen HJC, Postma JPM, Gunsteren WF, et al. Molecular dynamics with coupling to an external bath. J Chem Phys. 1984;81:3684-90.
17. Torrie GM, Valleau JP. Nonphysical sampling distribution in Monte Carlo free-energy estimation: umbrella sampling. J Comput Phys. 1977;23(2):187-99.
18. Kirkwood JG. Statistical mechanics of fluid mixtures. J Chem Phys. 1935;3(5):300-13.
19. Kumar S, Bouzida D, Swendsen RH, et al. The weighted histogram analysis method for free-energy calculations on biomolecules.1. The method. J Comput Chem. 1992;13(8):1011-21.
20. Roux B. The calculation of the potential of mean force using computer simulations. Comput Phys Commu. 1995;91(1-3):275-82.
21. Huang X, Zhao X, Zheng F, Zhan CG. Cocaine esterase-cocaine binding process and the free energy profiles by molecular dynamics and potential of mean force simulations. J Phys Chem B. 2012;116(10):3361-8.
22. Zhang YX, Huang X, Han KL, et al. Free energy profiles of cocaine esterase-cocaine binding process by molecular dynamics and potential of mean force simulations. Chem Biol Interact. 2016;259(B):142-7.

Citation of this Article

Xin L and Xinguan T. Exploring the Mechanism of the Cystic Fibrosis Transmembrane Conductance Regulator-ATP Binding Through Molecular Dynamics and Potential of Mean Force Simulations. Mega J Case Rep. 2022; 5: 2001-2015.

Copyright